

Response to reviewer 2's comments for Operational performance of the Vaisala CL61 ceilometer for atmospheric profiling

Viet Le¹, Ewan J. O'Connor¹, Maria Filioglou², and Ville Vakkari^{1,3}

¹Finnish Meteorological Institute, Helsinki, 00101, Finland

²Finnish Meteorological Institute, Atmospheric Research Centre of Eastern Finland, Kuopio, Finland

³Atmospheric Chemistry Research Group, Chemical Resource Beneficiation, North-West University, Potchefstroom, 2520, South Africa

Correspondence: viet.le@fmi.fi

We would like to thank the reviewers for the constructive comments. Below are the reviewer comments in black text, followed by our responses in [blue text](#). Where applicable, we also provide changes to the manuscript in *blue italics*.

1 General comments

This manuscript presents a long-term evaluation of the Vaisala CL61 depolarization ceilometer using measurements from four
5 ACTRIS Cloudnet sites in Finland and Germany. The study addresses several important aspects of the operational performance of this new-generation ceilometer, including background noise characterization, laser power degradation, temperature-dependent instrument bias, calibration stability, and the retrieval of aerosol backscatter and depolarization profiles.

The topic is timely and relevant. Depolarization-capable ceilometers are increasingly used in operational networks, and the CL61 represents an important step toward extending ceilometer applications to aerosol typing and cloud microphysics. A
10 careful characterization of instrument performance under long-term operation is therefore essential for both operational and research communities. The manuscript contains several interesting aspects, such as the use of termination hood measurements to quantify instrumental noise and the comparison of cloud and Rayleigh calibration approaches.

Overall, the manuscript is reasonably well structured and generally clear, although the organization could be improved in some parts. Several methodological aspects require clarification, and some conclusions appear stronger than what is fully
15 supported by the presented evidence. I therefore recommend publication after major revisions addressing the points outlined below.

[We would like to thank the reviewer for their positive evaluation of the manuscript.](#)

2 Specific comments

The manuscript would benefit from a clearer separation and description of the different signal components relevant to lidar
20 measurements (true atmospheric signal, background signal, instrumental dark signal) and their associated noise contributions in the methods section. It should also be clarified which components are corrected by the instrument firmware and which

require additional processing addressed in this study. The lidar equation presented in Section 2 would be more appropriately placed in this part of the paper.

The background definition B has been improved. Now it consists of estimated background signal $B_{estimated}$ by the instrument and residual background signal B_{res} . The residual background signal consists of atmospheric background signal (such as solar) and instrumental background signal (dark signal). The study examines the instrumental background signal and its associated noise. The atmospheric background signal has been corrected by the firmware, its variance (atmospheric background noise) will be addressed in this study.

Here are the updated paragraphs across the manuscript:

$$30 \quad ppol = \parallel \frac{(P(r) - B_{estimated})r^2}{C_{LO}(r)} = \parallel \beta', \quad (1)$$

$$xpol = \perp \frac{(P(r) - B_{estimated})r^2}{C_{LO}(r)} = \perp \beta', \quad (2)$$

where $B_{estimated}$ is the internally estimated background signal by the instrument.

...Although the instrument already determines and performs the background correction internally, residual background components may still remain in the measured signal, such as the dark signal observed during termination hood measurements (see Sect 3.1.1). Therefore, we extend Eqs. 2 and 3 to account for the residual background signal (hereafter referred to as the background signal), B_{res} , that is not removed by the internal correction:...

...Therefore, the firmware must have corrected the atmospheric background signal to a zero mean, leaving only its variance (noise) contributing to the background signal, which will be addressed in this study...

...During the termination hood measurement, $\mu_{P_{instrument}O(r)}$ from both polarizations remains relatively stable above 1.2 km, but increases significantly below this range (Figs. 3d, e). This increase suggests the presence of a signal bias at lower ranges that has not been corrected by the firmware and will be investigated in this study...

In addition, a clearer distinction between signal and noise is required throughout the manuscript, as these terms are occasionally used interchangeably, which may lead to confusion.

Thanks, this has been incorporated into the manuscript. An example is shown in lines 172-173:

45 Hence, the instrumental background signal mean (bias) and its variance (noise) from both polarizations with respect to internal temperature can be determined.

It is currently not clear whether the instrumental correction (dark signal) is negligible when compared to real atmospheric measurements. The manuscript would benefit from a quantitative assessment of the magnitude of the instrumental signal relative to the atmospheric signal, as well as a discussion of whether this contribution can be neglected and over which range.

50 Thanks, the following plots have been added to the supplements. Additionally, additional text to describe this is included in the manuscript.

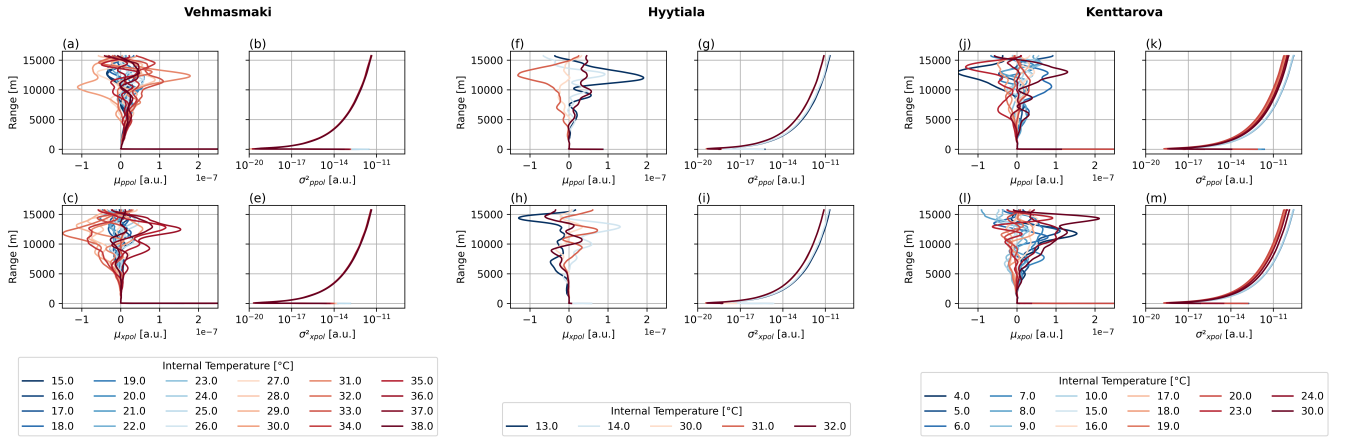


Figure S4. Termination hood profiles at various internal temperatures (color-coded) across different sites. In Vehmasmaki: a) μ_{ppol} , b) σ_{ppol}^2 , c) μ_{xpol} , and d) σ_{xpol}^2 . In Hyytiala: f) μ_{ppol} , g) σ_{ppol}^2 , h) μ_{xpol} , and i) σ_{xpol}^2 . In Kenttaroava: j) μ_{ppol} , k) σ_{ppol}^2 , l) μ_{xpol} , and m) σ_{xpol}^2

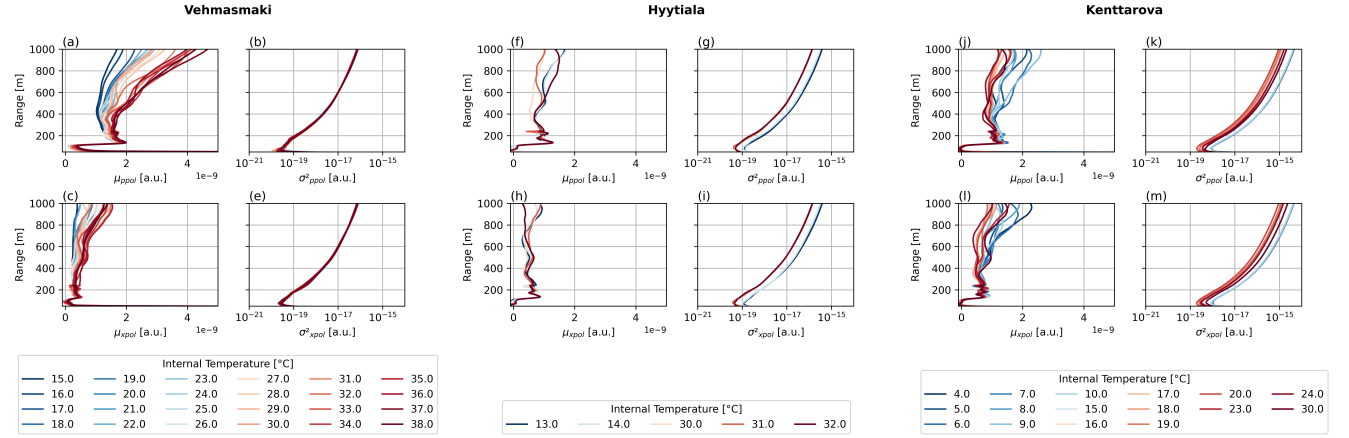


Figure S5. Termination hood profiles at various internal temperatures (color-coded) across different sites only up to 1000 m range. In Vehmasmaki: a) μ_{ppol} , b) σ_{ppol}^2 , c) μ_{xpol} , and d) σ_{xpol}^2 . In Hyytiala: f) μ_{ppol} , g) σ_{ppol}^2 , h) μ_{xpol} , and i) σ_{xpol}^2 . In Kenttaroava: j) μ_{ppol} , k) σ_{ppol}^2 , l) μ_{xpol} , and m) σ_{xpol}^2 .

Similar to Figs. 6 and 7, Figs. S4 and S5 show the same profiles obtained during the termination hood measurements, but include range correction and the instrument-provided overlap correction. These profiles of ppol and xpol provide a direct quantification of the impact of instrumental background bias and noise on the measurements and their dependence on temperature. For all CL61 instruments, the instrumental biases, μ_{ppol} and μ_{xpol} , remain below the order of 10^{-7} , while the noise terms, σ_{ppol}^2 and σ_{xpol}^2 , remain below the order of 10^{-11} . These biases are even smaller below 5 km. Below a range of 1 km, μ_{ppol} remains below 5×10^{-9} and μ_{xpol} below 3×10^{-9} . These small biases are usually negligible comparing to the typical atmospheric signal. However, at very clean sites such as Kenttaroava, the instrumental bias in xpol can still affect

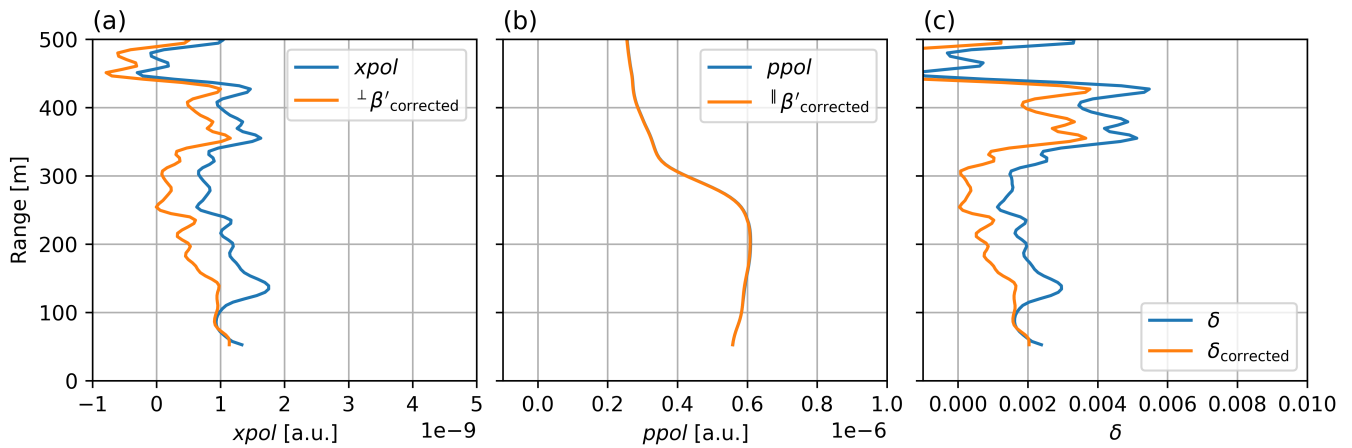


Figure S6. Data from Kenttäröva 2023-10-03, averaged from 11:00 to 15:00 UTC showing a) x_{pol} , b) p_{pol} c) δ .

the retrieved aerosol depolarization ratio, particularly under conditions of low depolarization. An example is shown in Fig. S6, which presents measurements from Kenttäröva on 2023-10-03 under weakly depolarizing aerosol conditions. During this period, the x_{pol} profile below 400 m is on the order of 10^{-9} , while p_{pol} remains on the order of 10^{-6} . As a result, the instrumental bias becomes relatively significant for x_{pol} , leading to a noticeable, although quantitatively small, reduction in δ (from 0.002 to 0.001 at 200 m) after the bias correction is applied. Furthermore, the previously mentioned peak at 150 m is clearly visible in this case and is effectively mitigated after the removal of the instrumental bias.

Some statements, for example regarding the recommended frequency of termination hood measurements, are not clearly supported by the presented results. This information would be particularly important for instrument operators, given the associated effort.

We modified our suggestion as following:

Figure 8 shows how the instrumental bias during the termination hood measurement at Vehmasmäki varies over time under consistent internal temperature conditions. Over a six-month period, the calibration profiles at each temperature show only minor fluctuations. Therefore, we recommend performing termination hood checks at least once across the operating temperature range to determine the instrumental background signal bias and noise.

In addition, the temperature-dependent overlap behaviour mentioned in the conclusions cannot be clearly inferred from the data shown.

As also noted by referee 1, we modified it to be the temperature dependence of the instrumental background bias and noise. This temperature dependence is shown in Fig. 6 and Fig. 7, and even more clearly in Fig. S4 and Fig. S5 below 1 km without the range and overlap correction.

Termination hood measurements were performed on selected instruments and proved effective in characterizing the instrumental background bias and noise profiles and their temperature dependence.

80 3 Technical comments

Line 1: Within the community, the term ALC has become established as standing for ‘Automatic Low-Power Lidar and Ceilometer’ or ‘Automatic Lidar-Ceilometer’. Perhaps the authors also wish to use this term to distinguish them from aerosol high-power lidars (AHL).

Thanks, we will follow the suggestion.

85 *The Vaisala CL61 is a new generation elastic backscatter lidar that extends conventional Automatic Lidar-Ceilometer capabilities by providing depolarization ratio measurements.*

Line 4: In this context, the focus should not be placed on the introduction of methods, as these are already well established in the lidar community, but rather on the adaptation and application of existing methods to long-term CL61 data, which represents a key contribution of this manuscript.

90 Changed the sentence to emphasize on the assessment of the CL61s.

In this study, performance of multiple CL61 instruments across different sites over 3 years period have been assessed.

Line 6: Does this refer to an increase in noise due to e.g. changes in detector characteristics or a decrease in the signal-to-noise ratio due to weaker return signals?

95 It is due to a decrease in signal-to-noise ratio due to weaker return signals, and the instrument’s compensation via internal calibration factor

Results indicate some differences between instruments, with most of these early production units exhibiting a pronounced decrease in laser power over time, accompanied by an increase in background noise likely due to weaker return signal

Line 11: A variation is obvious for the instrumental noise but is it also true for the bias?

100 Yes, it is. An example is in Fig. 7f and 7h, where cold temperature introduces negative bias in the near range. This is even more clear in the newly added Fig. S4 and Fig. S5.

Line 13: A commonly used term would be the particle backscatter coefficient and the particle linear depolarization ratio (PLDR).

Thanks, i will follow the suggestion.

105 *Additionally, an approach to estimate the uncertainty propagation of volume and particle backscatter and linear depolarization ratio is presented.*

Line 17: The correct wavelength of the CL61 according to the manual is 910.55 nm.

Thanks, i will follow the suggestion.

110 *This demonstrates the importance of accounting for the molecular contribution in both volume backscatter and linear depolarization ratio when qualitatively interpreting aerosol measurements by the CL61 Automatic Lidar-Ceilometer operating at the wavelength of 910.55 nm.*

Line 23: Shouldn’t it be attenuated

Yes, it is attenuated backscatter as shown in the manuscript.

Line 28: An essential point here is eye-safety

Thanks, i will follow the suggestion.

115 *Their ability to operate autonomously and reliably in challenging environmental conditions, as well as being eye-safe, makes them well-suited for long-term monitoring and integration into operational networks of national meteorological services and research institutions...*

Line 33: volume linear depolarization ratio (VLDR) δ_v

Thanks, i will follow the suggestion.

120 *Vaisala has recently introduced the CL61 ceilometer which is an ALC with the capability of measuring the volume linear depolarization ratio, δ_v , which is the ratio of the perpendicular to the parallel component of the backscattered signal relative to the emitted polarization.*

Line 46: As lidars have a blind zone or a difficult to correct range of incomplete overlap, it is in principle impossible to obtain reliable data all the way down to the surface.

125 *With monostatic systems such as the CL61 reliable data can be extended much closer to surface compared to most research-grade lidars. Here, we consider surface as heights that can be covered with standard masts, i.e. 50 - 100 m above ground.*

Identifying and correcting such artifacts in the CL61 would enable reliable observations extending down to heights that overlap with surface-based observations.

Line 50: Is it the optical path or rather the detector or transmitter unit which is temperature dependent?

130 *We think it is the combinations of those. Hence, we rephrase the sentence to say it is due to temperature dependent of the instrumental background signal as:*

Our analysis focuses on the impact of laser power on signal quality, the temperature sensitivity of the instrumental background,..

135 *Table 1: An additional important information is the telescope field of view and the height of complete overlap or the blind zone which is shortly mentioned in the text.*

Thanks, i will follow the suggestion. I added Fig. S1 about the overlap function in the supplement and added description in the text:

140 *The overlap functions are shown in Fig. S1. Full overlap between the transmitted laser beam and the receiver field of view is achieved at approximately 250 m range for the instrument at Kenttäröva. The instruments at Vehmasmaki and Hyytiälä have different overlap functions, with approximately 95% overlap at 250 m range and complete overlap at approximately 550 m range. The overlap function is reported only in the new firmware data and remains constant throughout the period. No overlap function was reported for the instrument at Lindenberg.*

Line 59: The manual states: attenuating acquisition for both signals with measurement time of 0.2 s and same receiver module is used for both signals. This means that receiver sensitivity calibration is not necessary.

145 *Thanks, this information has been added to the text as suggested:*

The CL61 alternates the acquisition of each polarization every 0.2 s, while using the same receiver module for both channels. Consequently, receiver sensitivity calibration is not required.

Line 71: pulses of linear polarized laser light

Thanks, i will follow the suggestion.

150 *In brief, the CL61 utilizes an InGaAs diode laser that emits linearly polarized pulses with an energy of 3.9 μJ at a repetition rate of 9.5 kHz*

Line 73: Is B the background noise or the sum of additional signal terms like background and dark signal?

The B term is the sum of all the background components in this equation. The B term has been clarified later as estimated background signal by the instrument $B_{estimated}$ and residual background signal B_{res}

155 Line 88: linear depolarization ratio

Thanks, i will follow the suggestion.

and the volume linear depolarization ratio being:

Line 92-94: In line 4, it was referred to as a background signal, which is more accurate, as the background signal does indeed have a mean value and is not merely noise.

160 Thanks, i will follow the suggestion and make the term noise and signal more clear throughout the whole text. Please see the previous reply in the Section 2 of this reply regarding this.

Line 94: Authors should clearly distinguish between the components of the measured lidar signal and label them correctly. The measured signal consists of the true atmospheric signal plus the background signal, which may be caused by solar radiation, but also by moonlight or artificial light. Added to this is the instrument-specific signal, which may also be referred to as the 'dark signal' and can be determined, for example, through termination hood measurements.

165

Thanks, i will follow the suggestion and make the term noise and signal more clear throughout the whole text. Please see the previous reply in the Section 2 of this reply regarding this.

The true atmospheric signal consists of backscattered contributions from particles (β_p) and molecular scattering (β_{mol}), whilst the background signal includes contributions from both atmospheric background signal $P_{atmosphere}$ (such as solar radiation, moonlight, or artificial light) and instrumental background $P_{instrument}$ signal (dark signal).

170

Line 95: The firmware already subtracts the background signal, but not the dark signal. Do the authors also assume that the background signal was not correctly determined and subtracted? If so, they should refer to it as the residual background signal and dark signal (determined with termination hood measurements).

Thanks, I will follow the suggestion and refer to it as the residual background signal. As explained in a later section, the atmospheric background signal was assumed to have been correctly determined and corrected. However, the atmospheric background noise remains present and is incorporated with the instrumental background noise into the uncertainty estimation.

175

Line 97: Can B_{bk} be described as the dark signal in this context?

This has been clarified in the text. The total background signal is B , of which the estimated background from the instrument is $B_{estimated}$ and the residual background signal is B_{res}

180 *...where $B_{estimated}$ is the internally estimated background signal by the instrument...*

...Therefore, we extend Eqs. 2 and 3 to account for the residual background signal (hereafter referred to as the background signal), B_{res} , that is not removed by the internal correction:...

Line 105: Background signal is usually range independent and dark signal range dependent. Since the solar component is specified here, is this then an uncorrected residual component?

185 No, the solar background signal mean is zero; however, the solar background noise remains substantial and is used to estimate the uncertainty, as shown in Eqs. 12–15.

Figure 1: Have σ and η for ppol and xpol been introduced yet?

Thanks, this has been added.

190 *During daylight hours, solar radiation significantly increases the variance (σ_{ppol/r^2}^2 and σ_{xpol/r^2}^2) of the background signal, resulting in a daytime variance much higher than that observed at night, as shown in panels (g) and (h). Above the aerosol and cloud layers, both the mean (μ_{ppol/r^2} and μ_{xpol/r^2}) and variance of the background signals in both polarizations remain relatively stable with range, or at least exhibit considerably smaller variations compared to the diurnal fluctuations.*

Line 131: To obtain the correct dark signal the overlap correction must be removed. It is still applied in the firmware but is not necessary for termination hood measurements and will lead to signal distortions in the incomplete overlap range which can influence interpretation of these measurements.

195 We do agree that removing the overlap function can clarify the interpretation of the measurement. As a result, the figures have been updated to undo the overlap correction in the context of instrumental background signal. Another set of Figures S4 and S5 which include both range correction and overlap correction have been added to the supplement for better interpretation.

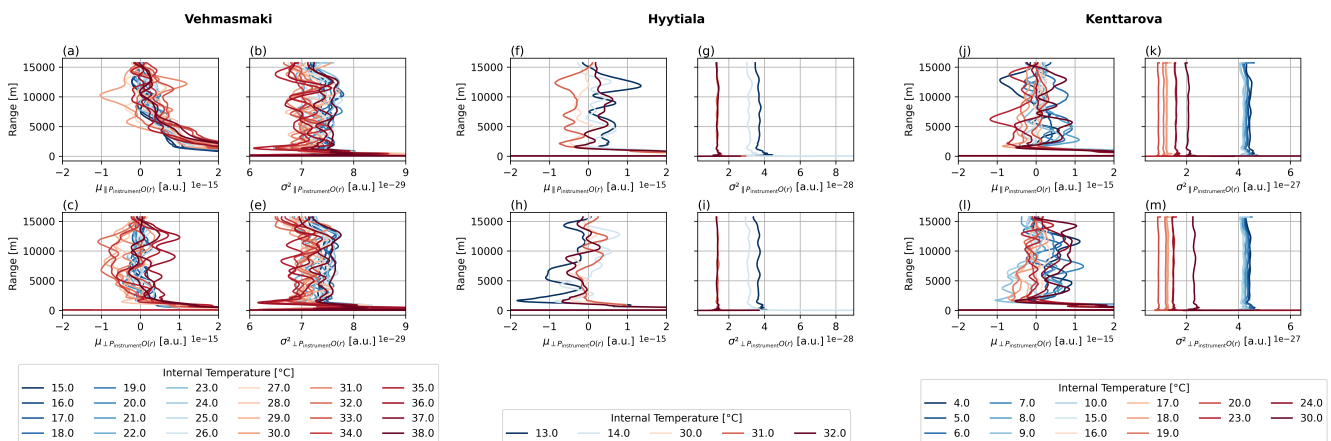


Figure 6. Termination hood profiles at various internal temperatures (color-coded) across different sites. In Vehmasmaki: a) $\mu_{\parallel P_{\text{instrument}} O(r)}$, b) $\sigma_{\parallel P_{\text{instrument}} O(r)}^2$, c) $\mu_{\perp P_{\text{instrument}} O(r)}$, and d) $\sigma_{\perp P_{\text{instrument}} O(r)}^2$. In Hyytiala: f) $\mu_{\parallel P_{\text{instrument}} O(r)}$, g) $\sigma_{\parallel P_{\text{instrument}} O(r)}^2$, h) $\mu_{\perp P_{\text{instrument}} O(r)}$, and i) $\sigma_{\perp P_{\text{instrument}} O(r)}^2$. In Kenttaroava: j) $\mu_{\parallel P_{\text{instrument}} O(r)}$, k) $\sigma_{\parallel P_{\text{instrument}} O(r)}^2$, l) $\mu_{\perp P_{\text{instrument}} O(r)}$, and m) $\sigma_{\perp P_{\text{instrument}} O(r)}^2$.

Line 135: β_{mol} is usually the molecular backscatter coefficient. What you rather should compare to find an aerosol-free region would be the hypothetical Rayleigh signal or β'_{mol} .

The details of the calculation could be provided already at this point and not in the next section.

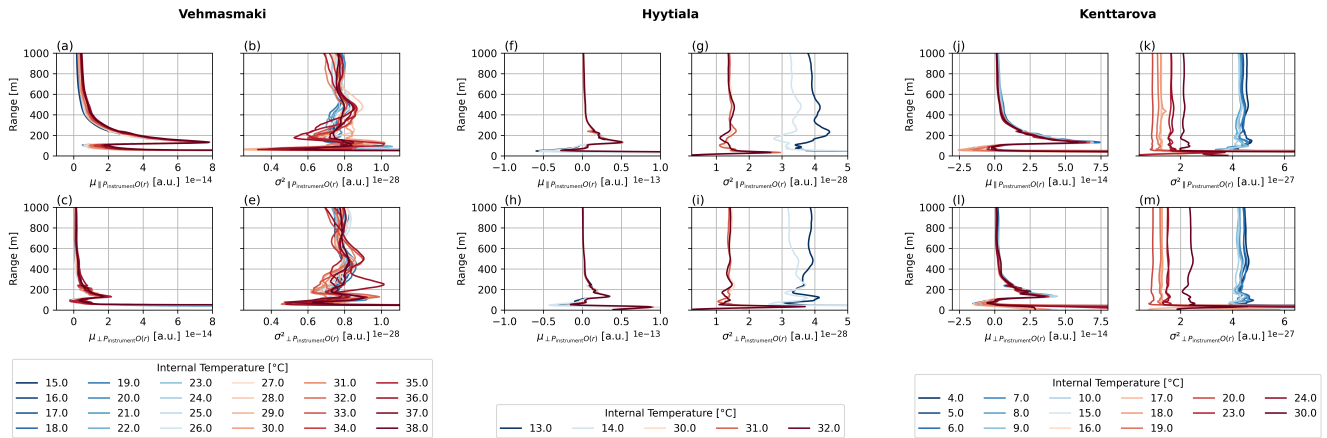


Figure 7. Termination hood profiles at various internal temperatures (color-coded) across different sites only up to 1000 m range. In Vehmasmaki: a) $\mu_{\perp P_{\text{instrument}}O(r)}$, b) $\sigma_{\parallel P_{\text{instrument}}O(r)}^2$, c) $\mu_{\parallel P_{\text{instrument}}O(r)}$, and d) $\sigma_{\perp P_{\text{instrument}}O(r)}^2$. In Hyttiala: f) $\mu_{\perp P_{\text{instrument}}O(r)}$, g) $\sigma_{\parallel P_{\text{instrument}}O(r)}^2$, h) $\mu_{\parallel P_{\text{instrument}}O(r)}$, and i) $\sigma_{\perp P_{\text{instrument}}O(r)}^2$. In Kenttaroova: j) $\mu_{\perp P_{\text{instrument}}O(r)}$, k) $\sigma_{\parallel P_{\text{instrument}}O(r)}^2$, l) $\mu_{\parallel P_{\text{instrument}}O(r)}$, and m) $\sigma_{\perp P_{\text{instrument}}O(r)}^2$.

Thanks, this has been implemented.

Before the termination hood was applied, the μ_{ppol} and μ_{xpol} profiles in the aerosol and hydrometeor-free region above 5 km closely follow the theoretical molecular attenuated backscatter coefficient β'_{mol} (Fig. 3b and c), indicating that the CL61 is sensitive to molecular scattering. The β'_{mol} profile was calculated following the method described by ? using meteorological input data from a numerical weather prediction model available from the ACTRIS Cloudnet data portal...

Line 147: See above. The overlap correction must be removed for the analysis. Perhaps the manufacturer can provide details if the correction is time dependent.

The instrument firmware applies a time-independent overlap correction to the measurements. It has now been removed from Figs. 6 and 7.

Line 148: Do you mean here "possible temperature dependence of the overlap function" instead of correction?

Thanks, this has been modified to explain that it is the instrumental background that has the temperature dependence.

It is likely that the observed bias is temperature-dependent and is caused by variations in instrumental background associated with afterpulsing, dark signal, and optical components under different temperature conditions

Line 149: Which temperature did you use? The CL61 measures laser_temperature, internal_temperature, and transmitter_enclosure_temperature.

internal_temperature was used. This clarification has been added to the text

To quantify the effect of temperature, the termination hood measurement was repeated over a range of internal temperatures T , reported as internal_temperature in the instrument housekeeping data, across a two-year period.

220 Line 153: Which diurnal pattern do you mean? Diurnal patterns are hardly visible in Fig. 3 (a) if only times from 11:00 until 16:00 are shown and only two hours are atmospheric measurements. In Fig. 1 (a) for instance, diurnal patterns are visible.

Thank you for spotting the mistake, it was meant to refer to Fig. 1.

The solar noise variance can be seen from the diurnal pattern in Fig. 1 and the difference between the σ^2 profiles before (Fig. 3f and 3g) and during (Fig. 3h and 3i) the termination hood measurement.

225 Line 162: Figure reference should be to Figure 3

Thank you for spotting the mistake, Fixed to refer to Fig. 3

Figure 3: The label in plot c) should be just β_{mol} .

Thank you for spotting the mistake, this is fixed

Line 168: Shouldn't a subscript "corrected" be added so that it isn't confused with Eq. 4?

230 Thanks, this has been implemented

$$\parallel \beta'_{\text{corrected}} = ppol - \mu_{\parallel P_{\text{instrument}}(r,T)} r^2, \quad (3)$$

$$\perp \beta'_{\text{corrected}} = xpol - \mu_{\perp P_{\text{instrument}}(r,T)} r^2, \quad (4)$$

Line 200: field of view should be added to Table 1

Thank you, this has been added

235 *Receiver field-of-view ± 0.56 mrad*

Line 215: What about the uncertainty in C which is not taken into account here? In line 224 you mention a 10% uncertainty. Did you average over several C values or have you applied a fit or trend with time between consecutive C values?

The C values were calculated on a monthly basis to ensure a sufficient number of data points for fitting within the theoretical range, while accounting for multiple scattering at different heights. Examples are provided in Figures S4 to S7 in the supplement.

240 *To ensure robust data fitting, the cloud calibration is performed monthly using all suitable liquid cloud observations detected from the methodology.*

Additionally, a revised equation incorporating a 10% uncertainty has been included.

The calibrated volume attenuated backscatter coefficient and its uncertainty can then be determined as follows, assuming the cloud calibration factor has an uncertainty of approximately 10% (Hopkin et al., 2019):

$$245 \quad \beta'_v = \beta'_{\text{corrected}} \cdot C, \quad (5)$$

$$\sigma^2_{\beta'_v} = (\sigma^2_{\beta'_{\text{corrected}}} + 0.01 \cdot \beta'^2_{\text{corrected}}) \cdot C^2. \quad (6)$$

For those instruments where termination hood measurements are not available:

$$\beta'_v = \beta' \cdot C, \quad (7)$$

$$\sigma_{\beta'_v} = (\sigma^2_{P_{\text{atmosphere}}} + 0.01 \cdot \beta'^2) \cdot C^2 = (\sigma^2_{\parallel P_{\text{atmosphere}}} + \sigma^2_{\perp P_{\text{atmosphere}}} + 0.01 \cdot \beta'^2) \cdot C^2. \quad (8)$$

250 Line 217: Termination instead of terminal

Thank you for spotting the mistake, this is fixed.

For those instruments where termination hood measurements are not available:

Line 228: S_p instead of S

Thank you for spotting the mistake, this is fixed.

$$255 \quad \sigma_{\beta_p}^2 = \left(\frac{\partial f}{\partial \beta'_v} \sigma_{\beta'_v} \right)^2 + \left(\frac{\partial f}{\partial C} \sigma_C \right)^2 + \left(\frac{\partial f}{\partial S} \sigma_{S_p} \right)^2. \quad (9)$$

Line 238: Termination instead of terminal

Thank you for spotting the mistake, this is fixed.

and δ_v is the volume linear depolarization ratio, which is $\delta_{\text{corrected}}$ in Eq. 17, or $\frac{x_{\text{pol}}}{p_{\text{pol}}}$ for instruments lacking termination hood measurements.

260 Line 241: Which NWP model was used here?

ECMWF IFS forecast was used, This has been added to the text

The input data for these calculations are taken from a numerical weather prediction model (ECMWF IFS forecast) provided via the ACTRIS Cloudnet data portal...

Figure 6: Please align subplots vertically. Subplot e) should be d) to be consistent with the caption.

265 Thank you, this is fixed. See Fig. 6 and 7 in this reply.

Line 305: Can this conclusion be drawn on the basis of three measurements taken over a period of six months, even though the last value is actually in the middle?

This would be an important conclusion for operators. This plot should be shown not only in the supplements.

We will modify the wording of this statement and bring the Figure to the main manuscript.

270 *Over a six-month period, the calibration profiles at each temperature show only minor fluctuations. Therefore, we recommend performing termination hood checks at least once across the operating temperature range to determine the instrumental background signal bias and noise.*

Section 4.4: Is a single profile shown or is an average over a time period discussed? What would be the influence on the uncertainty if averaged over several profiles? It would be nice to see profiles compared.

275 It shows a single profile. If multiple profiles were averaged, the uncertainty would be reduced by approximately a factor of \sqrt{n} , where n is the number of profiles, assuming each profile has similar uncertainty. Clarification regarding the figure is added, as well as an extra figure in the supplement showing the effect of averaging multiple profiles in 10 minutes.

Figure 10 presents the β , δ and their associated uncertainties in the aerosol layer below 1000 m obtained from a measurement profile recorded at 13:00 UTC on the same day.

280 *Averaging multiple profiles reduces the uncertainties, as illustrated in Fig. S13, which shows the profiles averaged over 10 minutes.*

To give a better idea, one could also mention some typical values for the depolarization ratio.

The following has been added:

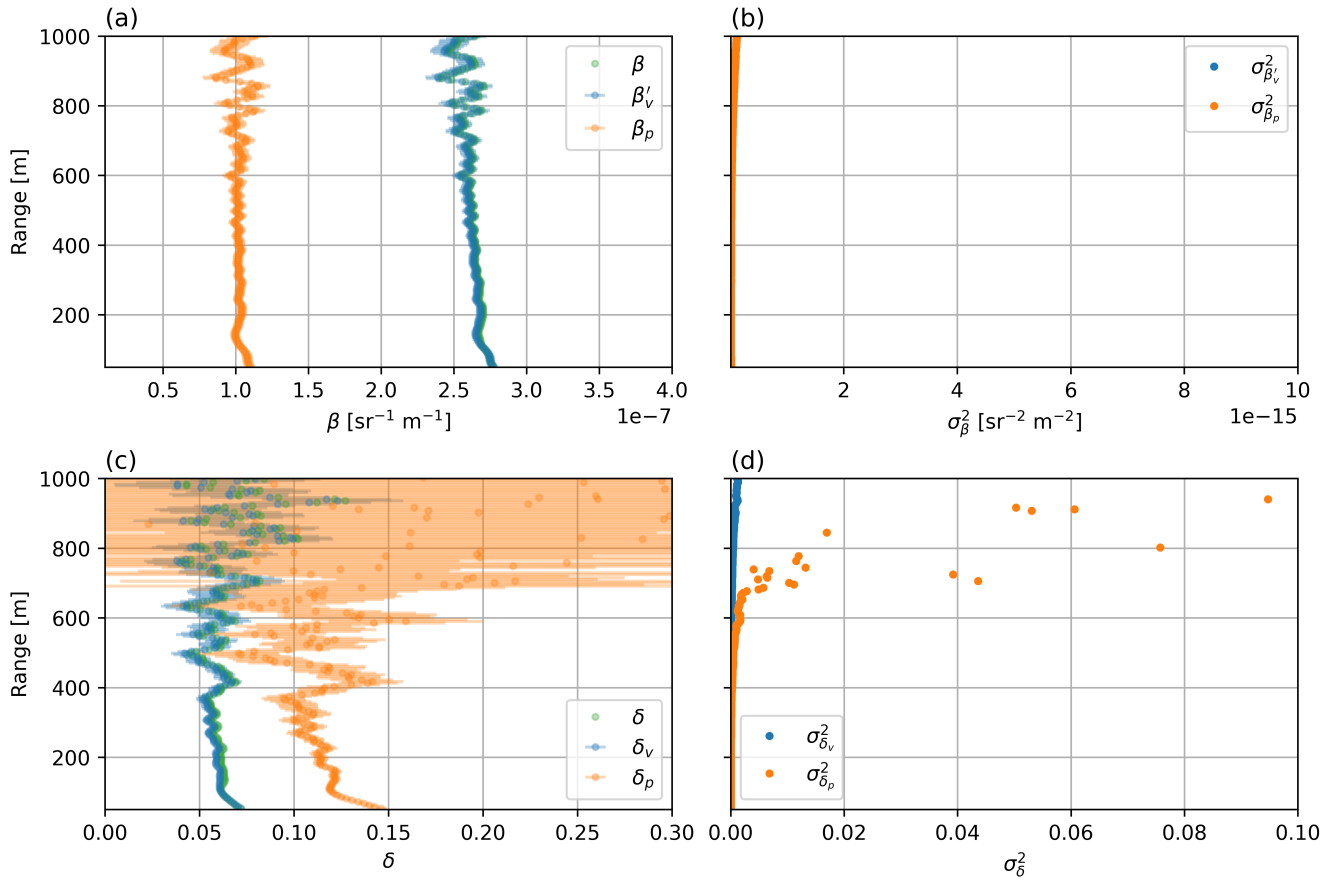


Figure S13. Example of uncorrected and corrected profiles in Kenttäröva, averaged from 2024-06-04 13:00 to 13:10 UTC. a) β , β'_v , β_p , b) $\sigma_{\beta'_v}^2$, $\sigma_{\beta_p}^2$, c) δ , δ_v , δ_p , d) $\sigma_{\delta_v}^2$, $\sigma_{\delta_p}^2$.

During pollen seasons in Finland, δ_p has been observed at 0.23 ± 0.06 for pine and 0.26 ± 0.06 for birch at this wavelength (Filioglou et al., 2023).

The authors might also consider plotting the various parameters as line plots, with the margin of uncertainty shown as a shaded area or error bars.

Thank you, this has been implemented

Line 349: Termination hood measurement

290 Thanks, it has been fixed

....the termination hood remains important as it allows the estimation of measurement uncertainty.

Figure 10: Why was for the subplots e)-h) another y-axis range chosen?

Because this is the result of the aerosol particle inversion, which focuses on the aerosol measurement. This has been added to the figure caption:

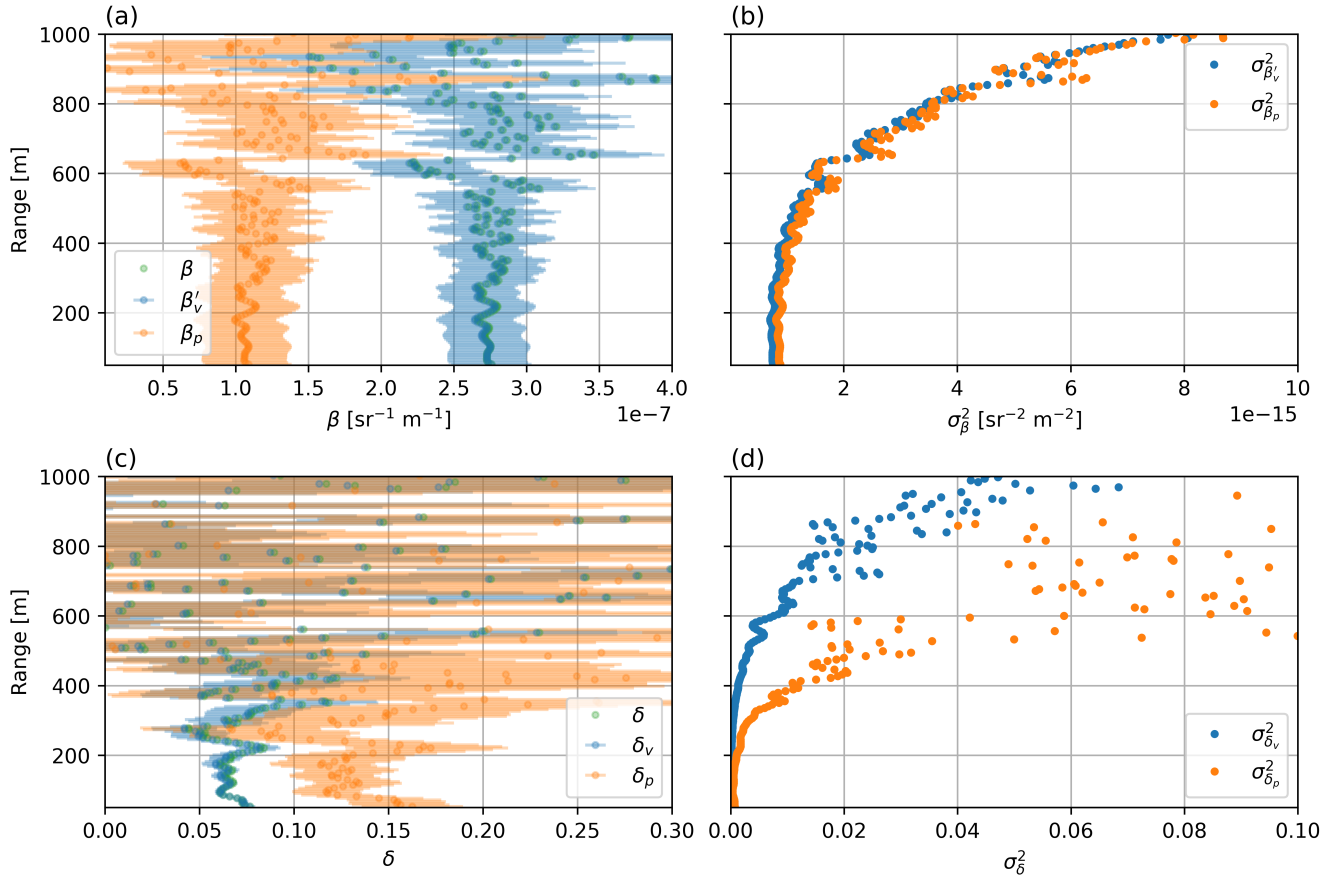


Figure 10. Example of uncorrected and corrected profiles in Kenttarova measured at 2024-06-04 13:01 UTC. a) β , β'_v , β_p , b) $\sigma_{\beta'_v}^2$, $\sigma_{\beta_p}^2$, c) δ , δ_v , δ_p , d) $\sigma_{\delta_v}^2$, $\sigma_{\delta_p}^2$.

295 *For particle properties in panels e-h, profiles are shown only up to 1 km range.*

Section 4.5: What was the reason for the high humidity inside the instrument? Was there a sealing problem with the window? Adding the relative humidity from the housekeeping data to the plot would help operators to see above which values this problem can happen.

We do not know the exact cause; it may be related to the window seal, although the problem persists even after its replacement. The relative humidity has been added to the Figure 12. However, the main issues here is that the condensation happens only at the window that is exposed to outside temperature while the relative humidity inside the instrument is still low. It can be thought of as a cold soda can in a room temperature. Condensation occurs at cold surface despite low relative humidity. We updated figure with internal relative humidity measurement and added a paragraph to the manuscript.

This occurred despite the measured internal relative humidity remaining below 70%. This is because the measurement does not represent the relative humidity at the window surface, where temperature is closer to ambient temperature.

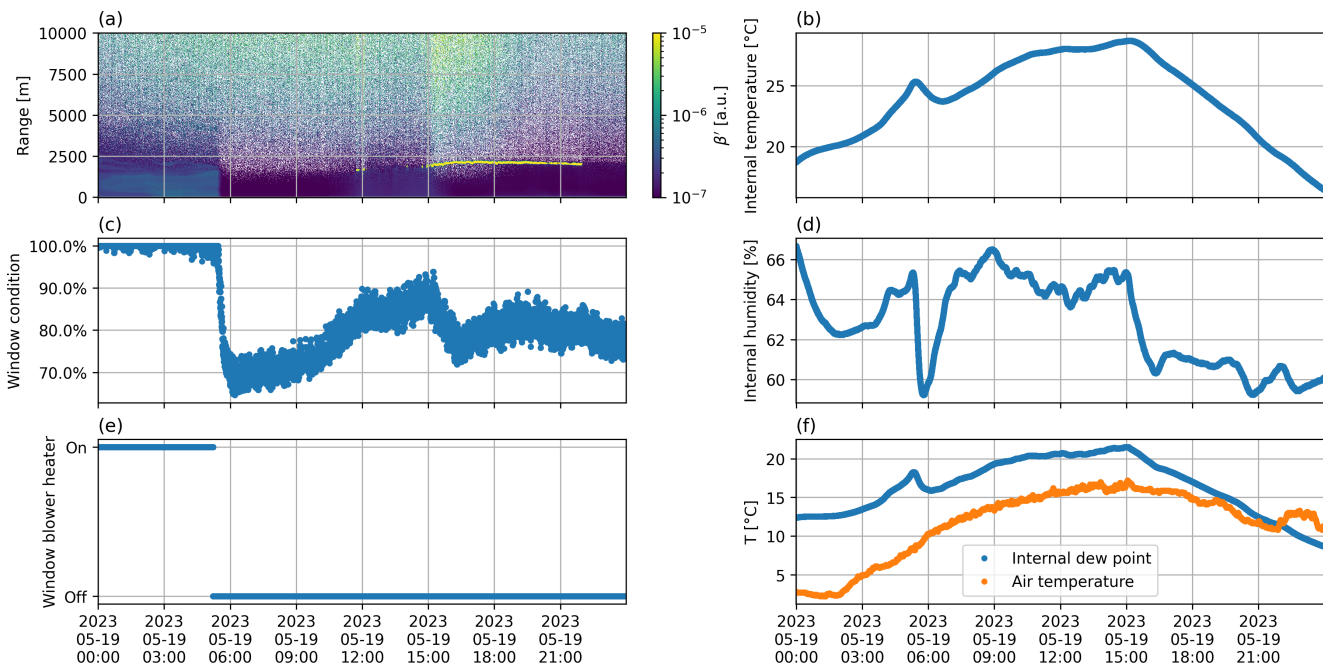


Figure 12. Measurements from Vehmasmäki on 2023-05-19 a) β' , b) Internal temperature, c) window condition, d) Internal humidity, e) Window blower heater, f) Calculated dew point and measured outside air temperature

Line 379: A temperature dependence of the overlap function was not clearly visible in Figure 7. Can this be stated here?

As also noted by referee 1, we modified it to be the temperature dependence of the instrumental background bias and noise. This temperature dependence is shown in Fig. 6 and Fig. 7, and even more clearly in Fig. S4 and Fig. S5 below 1 km without the range and overlap correction.

310 *Termination hood measurements were performed on selected instruments and proved effective in characterizing the instrumental background bias and noise profiles and and their temperature dependence.*

Line 384: See comment for line 305. The results in Figure S3 do not really support that conclusion here.

We have reconsidered the recommendation, and have reformulated it as follows:

315 *Over a six-month period, the calibration profiles at each temperature show only minor fluctuations. Therefore, we recommend performing termination hood checks at least once across the operating temperature range to determine the instrumental background signal bias and noise.*

Line 392: If quantitatively analyzing aerosol optical properties with lidar at this wavelength and at even longer wavelength, the molecular contribution must always taken into account. The difference in the backscatter coefficient is approximately the molecular backscatter coefficient at around 910 nm at ground level which can be calculated. Also the difference in is strongly dependent on the aerosol type and load and on altitude. It is not possible to make a general statement about the difference here, but it is clear that the molecular component must be taken into account.

320

We revised the text to emphasize the contribution of this study in presenting an approach for estimating measurement uncertainties using termination hood measurements. We also removed the general statement and made the conclusion regarding difference in depolarization ratio more specific to the low-aerosol conditions typically encountered in Finland.

325 *Nevertheless, the termination hood measurements remain crucial, as they allow the instrumental background to be quantified and subsequently used to estimate the uncertainties of β_p and δ_p , as presented in this study. For typical low aerosol load conditions in Finland, as in this study case, we found that the difference between β_p and β is approximately $1.5 \times 10^{-7} \text{ sr}^{-1} \text{ m}^{-1}$, and that between δ and δ_p is roughly 0.1 in the near surface layer.*

Line 395: Is it the fogging of the optical lens or the window?

330 It's the window, thanks for spotting the mistake

Additionally, some instruments experienced signal loss caused by the fogging of the window, which resulted in degraded data quality.

References

- Filioglou, M., Leskinen, A., Vakkari, V., O'Connor, E., Tuononen, M., Tuominen, P., Laukkanen, S., Toiviainen, L., Saarto, A., Shang, X., Tiitta, P., and Komppula, M.: Spectral dependence of birch and pine pollen optical properties using a synergy of lidar instruments, *Atmospheric Chemistry and Physics*, 23, 9009–9021, <https://doi.org/10.5194/acp-23-9009-2023>, 2023.
- Hopkin, E., Illingworth, A. J., Charlton-Perez, C., Westbrook, C. D., and Ballard, S.: A robust automated technique for operational calibration of ceilometers using the integrated backscatter from totally attenuating liquid clouds, *Atmospheric Measurement Techniques*, 12, 4131–4147, <https://doi.org/10.5194/amt-12-4131-2019>, 2019.